The role of rear release surfaces, block size and lateral confinement on rock slope failure mechanisms

Marc-André Brideau and Doug Stead
Earth Science Department, Simon Fraser University, Burnaby, BC, Canada

ABSTRACT
The importance of kinematic release mechanisms on translational slope failure is investigated using two- and three-dimensional distinct element codes. The role of the dip of the rear release surface and its influence on dilation and step-path failures is illustrated. Kinematic considerations due to varying lateral confinement/release mechanism are examined using two assumed three-dimensional slope models. The influence of block size on the calculated displacement and failure mechanisms in distinct element models is also studied.

RÉSUMÉ
L'importance des mécanismes de relâche cinématique sur les ruptures de pentes en translation fut étudiée en utilisant des codes bi- et tridimensionnels d'éléments distincts. Le rôle de l'angle de pendage de la surface de relâche arrière et son influence sur la dilatation et les ruptures en échelon sont démontrés. Les considérations cinématiques dues à la variation du confinement/relâche latérale sont examinées en utilisant deux modèles conceptuels de pente tridimensionnels. L'influence de la taille des blocs sur la valeur calculée des déplacements et des mécanismes de rupture dans la modélisation d'éléments distincts furent aussi étudiés.

1 INTRODUCTION

Kinematic analysis is usually the first stage in determining which failure mechanisms are feasible in a rock slope. This approach provides a rapid and easy first analysis which is an appropriate and necessary starting point. However, limitations of this technique include the lack of consideration of block size or shape and the influence of the presence and interaction of multiple discontinuity sets. This paper focuses on the implication of these limitations by undertaking a sensitivity analysis investigating the influence of:

i) the dip angle of the rear release discontinuity set
ii) the block size
iii) the degree of lateral confinement in 3-dimensions

on the failure mechanisms in a rock slope, using two- and three-dimensional distinct element codes. Planar sliding was selected as the primary failure mechanism investigated in this paper, since it is one of the simplest failure modes in rock slopes and because "sliding along an adversely orientated rock face or block edge will invariably occur if the kinematic conditions for such sliding are met" (Goodman and Kieffer, 2000). The sliding mechanism (on one- or two-planes) will be favoured over rotational movement if the geometry allows for a finite and removable block to form (Goodman, 2003; Goodman and Kieffer, 2000).

Previous work using distinct element codes to evaluate the sensitivity of the discontinuity set orientation on the failure mechanism was conducted by Kimber et al., (1998). In their study they varied the dip angle of the basal discontinuity set while keeping the dip angle of the rear release discontinuity constant. The failure mechanism was demonstrated to vary between sliding, sliding/toppling and toppling for different combinations. The aspect ratio of the blocks was also varied to show its influence on the failure mechanism (Kimber et al., 1998). The work presented in this paper provides a complementary study to the results presented by Kimber et al., 1998.

2 NUMERICAL MODELLING

The two- and three-dimensional distinct element codes, UDEC and 3DEC (Itasca, 2008a, b), were used in this paper due to their ability to model large displacement and rotation along block boundaries which allowed the sliding and toppling failure mechanisms to be modeled efficiently. The material type (rigid, elastic, or deformable) and its strength can be defined by the user. The shear and tensile strength along the block boundaries (discontinuities) can also be specified by the user. More information about the theory behind UDEC and 3DEC can be found in Cundall, (1976 and 1988), Hart et al., (1988) and Hart (1993). The material and discontinuity properties used in both distinct element codes are listed in Table 1.

The assumed rock slope profile investigated in UDEC is presented in Figure 1A. It consists of a 50 m high slope with a gradient of 66°. The dip angle of the basal (sliding) discontinuity set was kept constant at +30° while the dip angle of the rear release (toppling) discontinuity set was varied between -30° and +60° to investigate the sensitivity of the calculated displacement values and failure mechanisms to orientation. In the two-dimensional models (UDEC), the discontinuity spacing (block size) was also varied between 1, 2, 3 m and 6, 12, 18 m for the basal and rear release discontinuity respectively. This led to a constant block aspect ratio of (height: length) 1:6 and a tabular block shape. The block aspect ratio of 1:6 was deliberately chosen to favour a simple sliding failure mechanism according to the block shape stability charts proposed by Ashby (1971), Bray and Goodman (1981) and Sagaseta (1986).

The conceptual slope profiles investigated using 3DEC are presented in Figure 1B and C. The first model consist of the same cross-section used in the two-dimensional model but extended 100 m in the third dimension and bounded with assumed vertical and fixed lateral boundaries. The second 3DEC model has the same longitudinal cross-section but its lateral boundaries are assumed sloping and free. For these two 3-dimensional models the spacing (block size) was also varied between 1, 2, 3 m; 6, 12, 18 m; and 6, 12, 18 m for the basal, lateral release and rear release discontinuities respectively in order to investigate the scale effects on the calculated displacement values and failure mechanisms. This led to a constant block aspect ratio of (height:width:length) 1:6:6 and a tabular block shape.

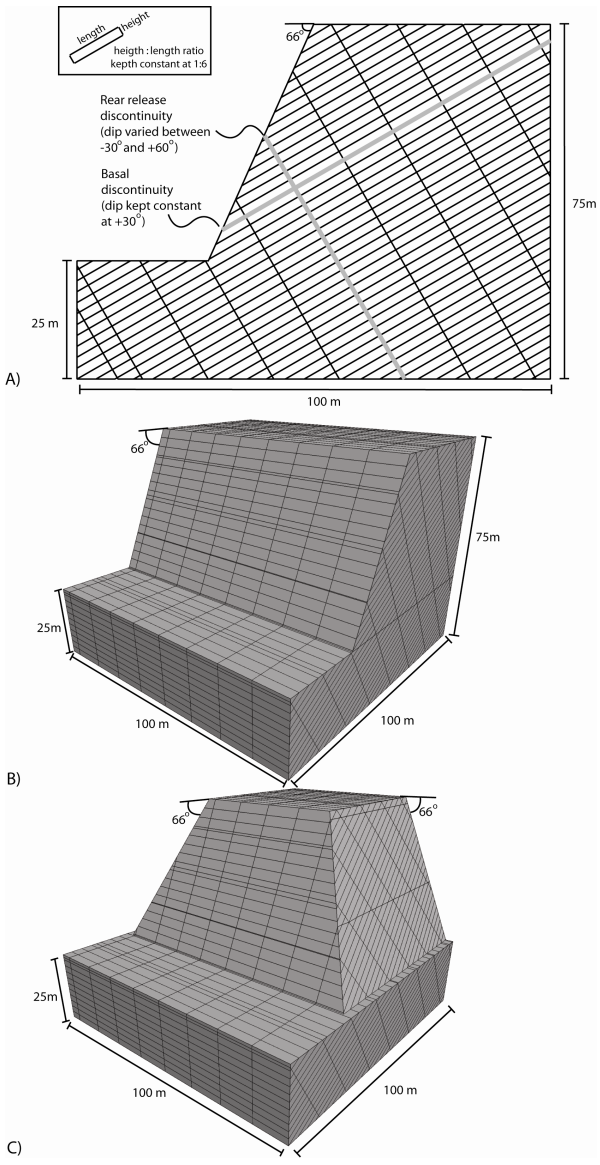

Figure 1. A) Geometry of the UDEC models investigated, B) geometry of the 3DEC models with assumed vertical and fixed lateral boundaries, C) geometry of the 3DEC models with assumed sloping and free lateral boundary

Table 1. Material and joint properties used in the UDEC and 3DEC models

Material properties	
Density (kg/m^3)	2700
Bulk modulus (GPa)	40
Shear modulus (GPa)	20
Joint properties	
Shear stiffness (GPa/m)	1
Normal stiffness (GPa/m)	10
Friction angle (^{o})	29
Cohesion (MPa)	0
Tensile strength (MPa)	0

3 RESULTS

The results from the different models investigated are summarized in Tables 2, 3, and 4.

3.1 Rear release dip in two-dimensional models

Table 2 shows that the failure mechanism in the two-dimensional models (UDEC) was controlled by the orientation of the rear release discontinuity and the size of the blocks. Figure 2 demonstrates that

- sliding at the toe and toppling in the slope crest area can be expected for a rear release discontinuity dip of -60^o
- "en-masse" sliding can be expected for a dip of 90^o
- a bi-planar failure mechanism for a dip of +60^o.

3.2 Block size in two-dimensional models

The influence of modeled block size on the failure mechanism is presented in Figures 3 and 4.

- the large (18x3m) block model with a basal discontinuity dip angle of +30^o and a rear release discontinuity dip of -70^o led to planar sliding failure (Figure 3A) while the small (6x1m) block model led to a slide-topple failure mechanism (Figure 3B)
- The large (18x3m) block model with a basal discontinuity dip angle of +30^o and a rear release discontinuity dip angle of +70^o led to a planar sliding failure (Figure 4A) while the small (6x1m) block model led to a bi-planar failure mechanism (Figure 4B).

In general, the results for the two-dimensional models (UDEC) show an overall trend (Table 3 and Figure 5) where the larger the block sizes result in larger calculated displacement values.

3.3 Three-dimensional modelling results

The discontinuity sets used in the 3DEC models investigated in this paper consisted of a basal discontinuity with an orientation of 30^o/270^o (dip/dd), a rear release discontinuity 60^o/090^o, and a lateral release discontinuity 90^o/000^o. The 3DEC models show the role of confinement (Fig. 6) and clearly demonstrated that sloping and free boundaries led to calculated maximum displacement two orders of magnitudes greater than the models with the assumed vertical and fixed lateral boundaries.

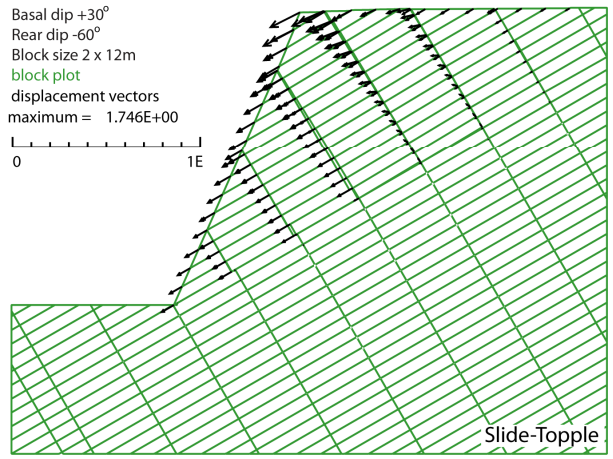

A)

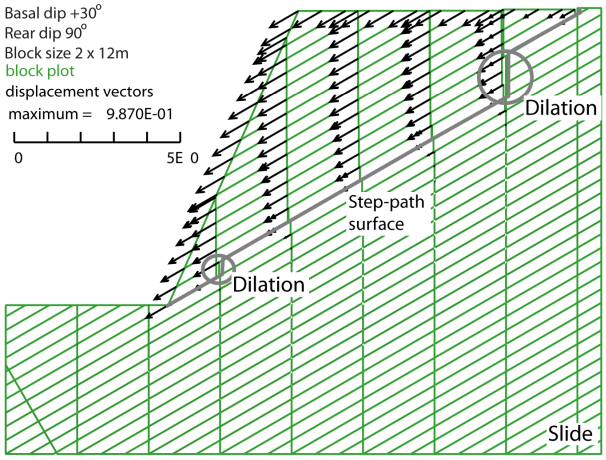

B)

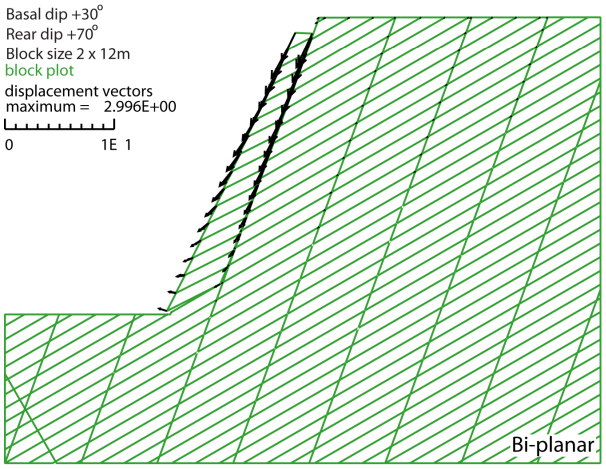

C)

Figure 2. Calculated displacement vectors obtained in the UDEC models (2x12m block size) with +30° dipping basal discontinuity set and a rear release discontinuity set dip angle of A) -60°, B) 90°, C) +70°

Table 2. Dominant failure mechanism obtained in the UDEC models as a function of the dip angle of the rear release discontinuity set and block size

Dip basal (°)	Dip rear (°)	Failure mode for model with 1x6m blocks	Failure mode for model with 2x12m blocks	Failure mode for model with 3x18m blocks
30	-30	Slide-topple	Slide-topple	Slide-topple
30	-40	Slide-topple	Slide-topple	Slide-topple
30	-50	Slide-topple	Slide-topple	Sliding
30	-60	Slide-topple	Slide-topple	Sliding
30	-70	Slide-topple	Sliding	Sliding
30	-80	Sliding	Sliding	Sliding
30	90	Sliding	Sliding	Sliding
30	80	Bi-planar	Sliding	Sliding
30	70	Bi-planar	Bi-planar	Sliding
30	60	Sliding	Sliding	Bi-planar

The results from 3DEC models where block sizes were varied (Table 4) showed larger calculated displacement when smaller block sizes were assumed. While the magnitude of the displacement was different, the movement type in the rock mass (2x12x12m) (Fig. 6) for both lateral boundary conditions (assumed vertical and fixed, sloping and free) indicated a toe sliding and toppling movement in the slope crest area. The failure mechanism as a function of lateral confinement (Table 4) also appears to be similar (sliding) for the 3x18x18m blocks. In contrast, three-dimensional models predict different failure modes (sliding for the assumed vertical and fixed; toppling for the sloping and free) for the 1x6x6m blocks. Table 4 suggests that block size can have an influence on the failure mechanism in three-dimensional numerical models.

4 DISCUSSION

In the numerical models where sliding and toppling both occurred (e.g. 2A, 3B, 6B and 6D), the sliding occurred in the lower portion of the model with toppling in the upper portion of the slope. These results are consistent with the limit equilibrium solution proposed by Goodman and Bray (1976) and could also be classified as slide head toppling according to the mass movement classification proposed by Goodman and Kieffer (2000). This mode of failure is regarded as a secondary toppling that occurs due to the "new" space created by the sliding block. The over-steepened toe needed for toppling to develop, as discussed by Nichol et al., (2002), is created by the sliding toe block. The bi-planar failures presented in Figure 2C and 4B have a back rotational component which corresponds to block slumping as described by Kieffer (2003, 2006) and Kinakin (2004). The unstable rock mass in the two-dimensional bi-planar failure models has a smaller area and different shape (columnar) than the sliding or slide-topple cases.

Using the two-dimensional distinct element code UDEC, Hencher et al., (1996) investigated the influence of block size on slope rock mass behaviour. They reported higher maximum displacement values for larger blocks, which is consistent with the results obtained in the UDEC models presented in this paper (Table 3). A study by Corkum and

Martin (2004) using 3DEC obtained higher displacement and volumetric dilation values as the number of blocks in their models was increased (i.e. smaller blocks). In the results presented in Table 4, similar results (smaller blocks leading to larger displacement) were obtained for the models with an assumed sloping and free lateral boundary. The apparently different scale effects for the maximum calculated displacement values between the two- and three-dimensional numerical models are emphasized. This may be due to the difference in geometry assumed in this paper and the work of Hencher et al., (1996) and Corkum and Martin (2004) or to the role of lateral confinement in 3-dimensional distinct element models. Further work on this aspect is required.

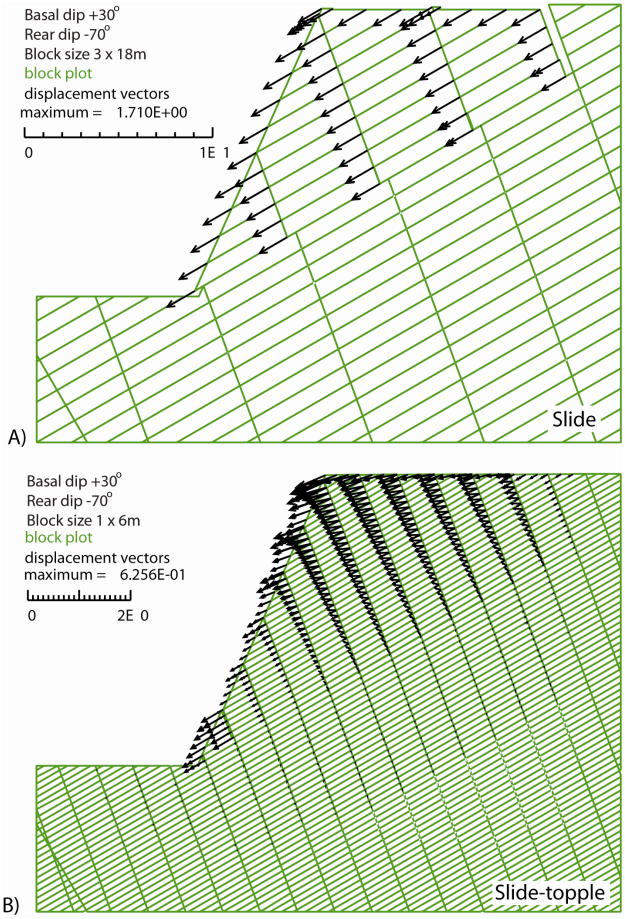

Figure 3. Calculated displacement vectors obtained in the UDEC models (basal discontinuity set dip angle +30°, rear release discontinuity set -70°) for block size A) 3x18m and B) 1x6m.

Hencher et al., (1996) also demonstrated that the failure mechanism was influenced by block size. They found for blocks with an aspect ratio of 1:1 (square), the sliding failure mechanism was simulated in models with smaller blocks while toppling occurred in models with larger blocks. The results presented herein indicate that sliding failure occurs when larger block geometries are assumed and that toppling dominates in models with smaller block (Table 2). This discrepancy was attributed to the tabular block shape used in this paper which facilitated a sliding mechanism for larger blocks.

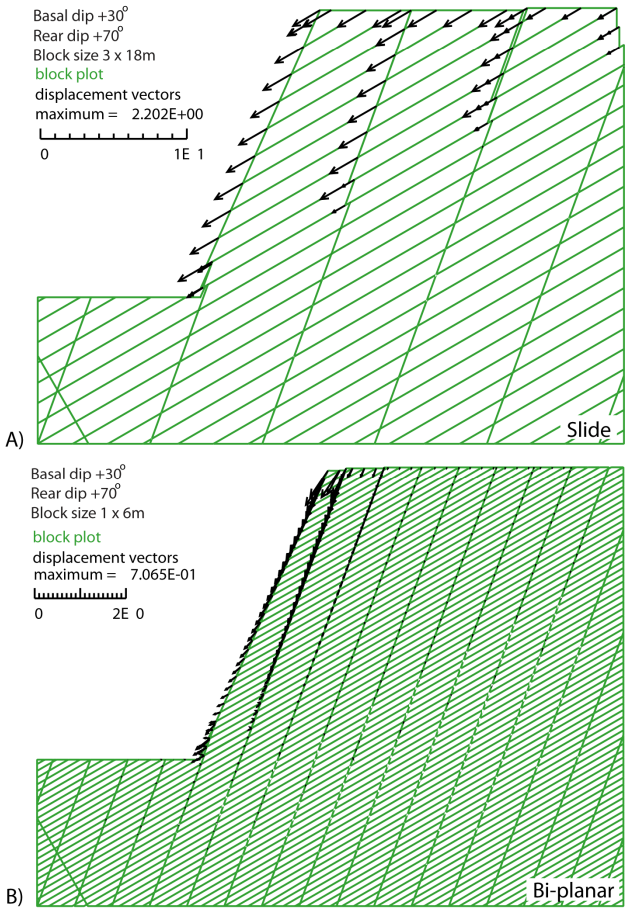

Figure 4. Calculated displacement vectors obtained in the UDEC models (basal discontinuity set dip angle +30°, rear release discontinuity set +70°) for block size A) 3x18m and B) 1x6m.

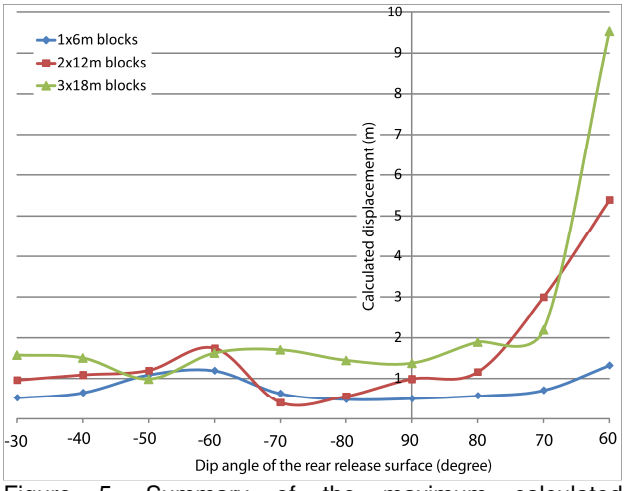

Figure 5. Summary of the maximum calculated displacement obtained in UDEC as a function of the rear release discontinuity set dip and block size.

Table 3. Dominant failure mechanisms obtained in the UDEC models as a function of the dip angle of the rear release discontinuity set and block size

Dip basal (°)	Dip rear (°)	1x6m blocks (displace-ment (m) after 30000 steps)	2x12m blocks (displacement (m) after 30000 steps)	3x18m blocks (displace-ment (m) after 30000 steps)
30	-30	0.52	0.96	1.58
30	-40	0.65	1.09	1.51
30	-50	1.09	1.20	0.99
30	-60	1.19	1.75	1.63
30	-70	0.63	0.40	1.71
30	-80	0.48	0.56	1.45
30	90	0.50	0.99	1.38
30	80	0.57	1.16	1.90
30	70	0.71	3.00	2.20
30	60	1.32	5.39	9.53

Table 4. Maximum calculated displacement and dominant failure mechanism in the 3DEC models as a function of block size and degree of lateral confinement.

Block size (HxLxW m)	Lateral boundaries	Displacement (m)	Failure mode
1x6x6	Vertical and fixed	0.14	Sliding
2x12x12	Vertical and fixed	0.11	Slide-topple
3x18x18	Vertical and fixed	0.14	Sliding
1x6x6	Sloping and free	32.39	Topple
2x12x12	Sloping and free	17.35	Slide-topple
3x18x18	Sloping and free	4.72	Sliding

Recent work by Galic et al., (2008) has investigated the role of confinement in physical models of sliding blocks on a multi-faced surface. They confirmed that increased lateral constraint in physical models leads to higher effective friction angles. The results presented in Figure 6 demonstrate that the expected displacement values from a slope with sloping and free lateral conditions can be two orders of magnitude greater than for a slope with vertical and fixed lateral boundary conditions. Just as in the experiments by Galic et al., (2008) these results are attributed to the dilation that can occur in the slopes (or blocks) with lesser degrees of lateral confinement. The conditions of assumed vertical and fixed lateral boundaries are thought to represent the geometry present along an open-pit bench, while the assumed sloping and free lateral boundaries would be more representative of a road cut through an isolated topographic high. Both of these situations are therefore feasible and the potential for rock mass dilation (such as with the sloping and free lateral boundaries) should be noted during site investigation and included in the slope stability analysis. Similar results were obtained by Palassi and Ashitiani (2008) who compared two- and three-dimensional distinct element models (UDEC and 3DEC). They found that the UDEC models had a higher factor of safety than the equivalent three-dimensional convex slope profile.

The development of step-path failure surfaces is generally associated with non-fully persistent discontinuity sets (Jennings, 1970; Einstein et al., 1983; Goodman, 2000) and it has been observed in laboratory experiments (Bobet and Einstein, 1998), numerical models (Eberhardt et al., 2004; Yan et al., 2007a,b; Franz and Cai, 2008) and in field studies (Yan, 2008; Brideau et al., 2009). The notion of step-path failure surface is also implicit in the analytical solution to block toppling by Goodman and Bray (1976). The results presented in this paper demonstrate that stepped-failure surfaces can also develop in models with fully persistent discontinuity sets. Figures 2B and 6D show the development of a step failure surface along the fully persistent basal discontinuity set. While the step-path failures rock masses with non-persistent discontinuities are the result from stress concentration and intact rock fractures, the step-paths in the models presented in this paper are due to rock mass dilation and discontinuous displacement along the fully persistent discontinuity sets. Development of these step-path failure surfaces were observed predominantly in the numerical models with larger block sizes (18x3m and 12x2m).

While the block aspect ratio (height to length) 1:6 used in this paper should have favoured a planar sliding failure mechanism, the results presented demonstrate that a toppling mechanism can occur in the 2- and 3-dimensional numerical models of a rock mass even when individual blocks have a tabular shape. This is attributed to the fully persistent nature of the rear release (toppling) discontinuity which can act as a single column when the rock mass is confined and/or the block size is small enough relative to the size of the slope. This phenomenon had been described previously by Aydan et al., (1989) for base friction physical models with fully persistent discontinuities. It is therefore suggested that classifications such as proposed by Ashby (1971) and toppling nomograms (Choquet and Tanon, 1985) should only be applied when investigating the stability of an individual rock block, a rock mass assuming discontinuities with limited persistence relative to the size of the slope of interest or when the blocks in the rock mass are relatively large compared to the slope of interest.

Finally, two other factors not considered in this paper that could also have influence on the shape, volume, and failure mechanisms of an unstable rock mass are the persistence of the discontinuity sets and varied strength (shear and/or tensile) along the different discontinuity sets in a given model. The role of limited persistence discontinuity was investigated in base friction physical models by Aydan et al., (1989) who found that limited persistence increased the stability field.

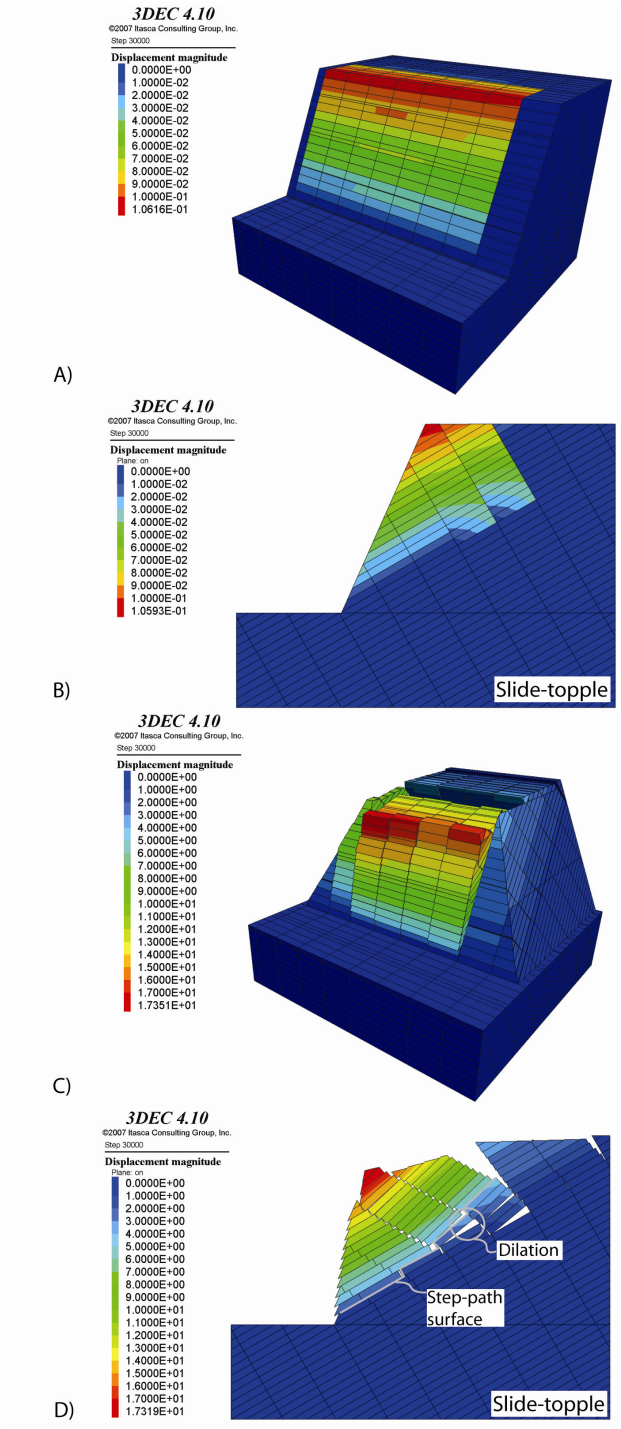

Figure 6: Calculated displacement contours in 3DEC (2x12x12m block size) with A) assumed vertical and fixed lateral boundary model, B) longitudinal cross section of the assumed vertical and fixed lateral boundary model, C) assumed sloping and free lateral boundary model, D) longitudinal cross-section of the assumed sloping and free lateral boundary model

The role of the discontinuity set persistence was also investigated by Franz (2008) using 3DEC to model the importance of the lateral and rear release discontinuity sets at the Cadia Hill Open Pit in Australia. He found that the extent of the unstable rock mass was influenced by discontinuity persistence (Franz, 2008). Work by MacLaughlin and Sitar (1999) and Sitar et al., (2005) has demonstrated using a Discontinuous Deformation Analysis (DDA) code that a toppling or sliding failure mechanism could be favoured in models with the same geometry with different friction angle on the discontinuity sets.

5 CONCLUSIONS

The influence of rear release discontinuity dip, block size and lateral confinement on planar sliding, toppling, and bi-planar failure mechanisms was investigated using two- and three-dimensional distinct element codes. Changes in the dip angle of the rear release discontinuity were found to have a marked influence on the dominant failure mechanism simulated in the models. Results suggest that the identification of a discontinuity set in the kinematic analysis which leads to a feasible planar failure mechanism for a finite and removable block might not be sufficient to assume that planar sliding will be the dominant failure mechanism. The interaction between the rear and lateral release surfaces also needs to be considered. Block size was shown to influence the failure mechanism in two- and three-dimensional numerical models. The influence of the block size on the calculated maximum displacement was found to be different between the two- and three-dimensional numerical models. This result was unexpected and warrants more investigation. Lateral confinement was found to have a marked influence on the calculated maximum displacement. The results of our research emphasize that it is important to consider basal, rear and lateral release surfaces when assessing the potential failure modes. A through-going basal joint set may result in planar, toppling, or bi-planar failure depending on the orientation of the rear release surface and block size.

ACKNOWLEDGEMENTS

The authors would like to acknowledge funding from NSERC and the FRBC Resource Geoscience and Geotechnics Endowment Fund. The authors would also like to thank D. Garagash for his review of the manuscript.

REFERENCES

Ashby, J., 1971. Sliding and toppling modes of failure in model and jointed rock slopes, M.Sc. thesis London University, Imperial College

Aydan, O., Shimizu, Y. and Ichikawa, Y., 1989. The effective failure modes and stability of slopes in rock mass with two discontinuity sets. Rock Mechanics and Rock Engineering, 22: 163-188.

Bobet, A., and Einstein, H.H., 1998. Fracture coalescence in rock-type material under uniaxial and biaxial compression. International Journal of Rock Mechanics and Mining Sciences. 35(7): 863-888.

Bray, J.W. and Goodman, R.E., 1981. The theory of base friction models. International Journal of Rock Mechanics and Mining Sciences & Geomechanics Abstracts, 18: 453-468.

Brideau, M.-A., Yan, M., and Stead, D., 2009. The role of tectonic damage and brittle rock fracture in the development of large rock slope failures. Geomorphology. 103(1):30-49.

Choquet, P. and Tanon, D.D.B., 1985. Nomograms for the assessment of toppling failure in rock slopes, 26th U.S. Symposium on Rock Mechanics. Balkema, Rotterdam, Rapid City, South Dakota, pp. 19-30.

Corkum, A.G. and Martin, C.D., 2004. Analysis of a rock slide stabilized with a toe-berm: A case study in British Columbia, Canada. International Journal of Rock Mechanics & Mining Sciences, 41(7): 1109-1121.

Cundall, P.A., 1988. Formulation of a three-dimensional distinct element model - Part I: A scheme to detect and represent contacts in a system composed of many polyhedral blocks. International Journal of Rock Mechanics and Mining Sciences & Geomechanics Abstracts, 25(3): 107-116.

Cundall, P.A., 1976. Computer interactive graphics and the distinct element method, Rock engineering for foundations and slopes. American Society of Civil Engineers, Boulder, Colorado, pp. 193-199.

Eberhardt, E., Stead, D. and Coggan, J.S., 2004. Numerical Analysis of Initiation and Progressive Failure in Natural Rock Slopes - the 1991 Randa Rockslide. International Journal of Rock Mechanics and Mining Sciences, 41(1): 69-87.

Einstein, H.H., Veneziano, D., Baecher, G.B. and O'Reilly, K.J., 1983. The effect of discontinuity persistence on rock slope stability. International Journal of Rock Mechanics, Mining Sciences and Geomechanic Abstract, 20(5): 227-236.

Franz, J., 2008. An investigation of combined failure mechanisms in large scale open pit slopes. PhD thesis. University of New South Wales, Sydney Australia

Franz, J., and Cai, Y., 2008. Investigation of slope failure mechanisms caused by large scale geological structures at the Cadia Hill Open Pit. In: Chen, Z., Zhang, J.-M., Ho, K., Wu, F.-Q., Li, Z.-K., (Eds.) Proceedings of the 10th International Symposium on Landslides and Engineered Slopes. P. 1165-1171

Galic, D., Glaser, S.D. and Goodman, R.E., 2008. Calculating the shear strength of a sliding asymmetric block under varying degrees of lateral constraint. international Journal of Rock Mechanics & Mining Sciences, 45(8): 1287-1305.

Goodman, R.E., 2003. A hierarchy of rock slope failure modes. Felsbau, 21(2): 8-12.

Goodman, R.E. and Bray, J.W., 1976. Toppling of rock slopes, Specialty Conference on Rock Engineering for Foundations and Slopes. American Society of Civil Engineering, Boulder, Colorado, pp. 201-234.

Goodman, R.E. and Kieffer, D.S., 2000. Behaviour of rock in slopes. Journal of Geotechnical and Geoenvironmental Engineering, 126(8): 675-684.

Hart, R.D., 1993. An introduction to distinct element modeling for rock engineering. In: J.A. Hudson, E.T. Brown, C. Fairhurst and E. Hoek (Editors), Comprehensive Rock Engineering: Principles, Practice and Projects. Pergamon, pp. 245-261.

Hart, R., Cundall, P.A., and Lemos, J., 1988. Formulation of a three-dimensional distinct element model – part II. Mechanical calculations for motion and interaction of a system composed of many polyhedral blocks. International Journal of Rock Mechanics, Mining Sciences, and Geomechanics Abstracts 25(3): 117-125.

Hencher, S.R., Liao, Q.-H. and Monaghan, B.G., 1996. Modelling slope behaviour for open-pits. Transactions of the Institution of Mining and Metallurgy Section A-Mining Industry, 105: A37-A47.

Itasca, 2008a. UDEC, Universal Distinct Element Code version 4.01. Itasca Consulting Group Inc. Minneapolis, Minnesota.

Itasca, 2008b. 3DEC version 4.10, Itasca Consulting Group Inc. Minneapolis, Minnesota.

Jennings, J.E., 1970. A mathematical theory for the calculation of the stability in open cast mines. Planning of Open Pit Mines Proceedings, Johannesburg, South Africa, pp. 87–102.

Kieffer, D.S., 2003. Rotational instability of hard rock slopes. Felsbau, 21(2): 31-38.

Kieffer, D.S., 2006. Influence of cross jointing on block slump stability, 41st US symposium on Rock Mechanics: 50 Year of Rock Mechanics - Landmark and Future Challenges, Golden, Colorado, pp. 06-1127.

Kimber, O.G., Allison, R.J. and Cox, N.J., 1998. Mechanisms of failure and slope development in rock masses. Transactions of the Institute of British Geographers, 23(3): 353-370.

Kinakin, D., 2004. Occurrence and genesis of alpine linears due to gravitational deformation in south western British Columbia. M.Sc. Thesis, Simon Fraser University, Burnaby, BC, 174 pp.

MacLaughlin, M.M. and Sitar, N., 1996. Kinematics of sliding on a hinged failure surface. In: H. Aubertin, Mitri (Editor), Rock Mechanics. Balkema, Rotterdam, pp. 2025-2030.

Nichol, S.L., Hungr, O. and Evans, S.G., 2002. Large-scale brittle and ductile toppling of rock slopes. Canadian Geotechnical Journal, 39: 773-788.

Palassi, M. and Ashitiani, M., 2008. Comparison of 2D and 3D distinct element analyses in stability of convex jointed rock slopes, 61st Canadian Geotechnical Conference and 9th Joint CGS/IAH-CNC Groundwater Conference. Canadian Geotechnical Society, Edmonton, AB, pp. 640-645.

Sagaseta, C., 1986. On the modes of instability of a rigid block on an inclined plane. Rock Mechanics and Rock Engineering, 19: 261-266.

Sitar, N., Maclaughlin, M. and Doolin, D.M., 2005. Influence of kinematics on landslide mobility and failure mode. Journal of Geotechnical and Geoenvironmental Engineering, 131(6): 716-728.

Yan, M. 2008. Numerical modelling of brittle fracture and step-path failure: from laboratory to rock slope scale. PhD thesis. Simon Fraser University, Burnaby, Canada.

Yan. M., Stead, D and Sturzenegger, M. 2007a. Step-path characterization in rock slopes: An integrated numerical modeling-digital imaging approach. In: Proceeding of the 11th Congress of the International Society for Rock Mechanics. Lisbon, Portugal. pp. 693-696.

Yan, M., Elmo, D. and Stead, D. 2007b. Characterization of step-path failure mechanisms: A combined numerical modelling-field based study. In: Proceeding of the 1st Canada-U.S. Rock Mechanics Symposium. Vancouver, BC. pp. 493-501.